TELKOMNIKA, Vol. 11, No. 4, April 2013, pp. 1797~1806
ISSN: 2302-4046

Adaptive RBFNN Formation Control of Multi-mobile Robots with Actuator Dynamics

Li Yan-dong*[1], Zhu Ling[2], Sun Ming[3]
[1, 2, 3]College of Computer and Control Engineering, Qiqihar University, Qiqihar, China
No.42, Wenhua Street, Qiqihar, Heilongjiang, China, 161006, (+086)0452-2738183
*Corresponding author, e-mail: liyandong1234@126.com

Abstract

We study the problem of formation control and trajectory tracking for multiple nonholonomic mobile robots with actuator and formation dynamics. An adaptive neural-network (NN) control strategy that integrated kinematic controller with input voltages controller of actuator was proposed. A control law was designed by backstepping technique based on separation-bearing formation control structure of leader-follower. The radial basis function neural network (RBFNN) was adopted to achieve on-line estimation for the dynamics nonlinear uncertain part for follower and leader robots. The adaptive robust controller was adopted to compensate modeling errors of NN. This strategy not only overcomed all kinds of uncertainties of mobile robots, but also ensured the desired trajectory tracking of robot formation in the case of maintaining formation. The stability and convergence of the control system were proved by using the Lyapunov theory. The simulation results showed the effectiveness of this proposed method.

Keywords*: formation control, multi-nonholonomic mobile robots, adaptive control, actuator dynamics, stability of nonlinear systems*

1. Introduction

There are several methodologies to robotic formation which include behavior-based [1], virtual structures [2],and leader-follower [3, 4] to name a few. Perhaps the most popular and intuitive approach is the leader-follower method. One characteristic that is common in many formation control schemes [5, 6] is the design of a kinematic controller to keep the formation. Which requires a perfect velocity-tracking assumption. Thus, where only velocity commands are treated, the stability of the formation is entirely dependent on the assumption that the robot perfectly tracks the designed control velocity. These controllers usually don't consider the dynamic characteristics of the robot, and lack robustness to the disturbance and the model uncertainty, and there are still many uncertainties in the practical application, like the role of noise in the mobile robot, the disturbance, the friction and load changes, etc in some of known dynamic model. To ensure that the robots are tracking expected speed and make formation error converges to zero, single robot and formation dynamics should be considered. In literal [7], the dynamics of the follower robot are considered and a neural network (NN) is introduced to estimate its dynamics; however, the dynamical effects of the leader and the formation are ignored. Through the Backstepping method and state feedback controller in [8], the formation dynamics is introduced into the design of the control input, and mobile robots (including friction) formation were studied through the introduction of the multilayer feedforward neural network, but it does not consider the formation robot suffered disturbance and load change. In most of the research works for formation control of mobile robot with dynamic, wheel torques are control inputs though in reality wheels are driver by actuators (e.g. DC motors) and therefore using actuator input voltages as control inputs is more realistic. For the formation control problem of multiple nonholonomic mobile robots with actuator and formation dynamics, this paper presented a drive voltage adaptive control based on radial basis function neural network (RBFNN).

The paper is organized as follows, section 2 describes the kinematic and dynamic model of WMR. In section 3, the leader-follower formation control problem is studied. Section 4 presents numerical simulations, and section 5 gives conclusions.

Received December 30, 2012; Revised February 7, 2013; Accepted February 19, 2013

2. Model

The mathematical model of nonholonomic mobile robots is as follows [9]:

$$\dot{\boldsymbol{q}} = \begin{bmatrix} \dot{x} \\ \dot{y} \\ \dot{\theta} \end{bmatrix} = \boldsymbol{s}(q)\boldsymbol{V} = \begin{bmatrix} \cos\theta & -d\sin\theta \\ \sin\theta & d\cos\theta \\ 0 & 1 \end{bmatrix} \begin{bmatrix} v \\ \omega \end{bmatrix} \quad (1)$$

$$\bar{\boldsymbol{M}}(q)\dot{\boldsymbol{V}} + \bar{\boldsymbol{C}}(q,\dot{q})\boldsymbol{V} + \bar{\boldsymbol{F}} + \bar{\boldsymbol{\tau}}_d = -a_1\bar{\boldsymbol{B}}\boldsymbol{X}\boldsymbol{V} + a_2\bar{\boldsymbol{B}}\boldsymbol{u} \quad (2)$$

Where $\boldsymbol{q} = (x, y, \theta)^T$ denotes the actual Cartesian position and orientation of the physical robot, R is the distance between the driving wheels and r is the radius of the wheel of the mobile robot, v and ω represent linear and angular velocities, respectively, and $\boldsymbol{V} = [v \quad \omega]^T$, the matrix $\bar{\boldsymbol{M}}(q)$ is a symmetric positive definite inertia matrix, $\bar{\boldsymbol{C}}(q,\dot{q})$ is the centripetal and Coriolis matrix, $\bar{\boldsymbol{B}}$ is a constant nonsingular matrix that depends on the distance between the driving wheels R and the radius of the wheel r, $\bar{\boldsymbol{\tau}}_d$ denotes bounded unknown disturbances including unstructured unmodeled dynamics, $\bar{\boldsymbol{F}}$ is the surface friction, $\boldsymbol{u} = [u_r \quad u_l]^T$, where u_r and u_l represent input voltage of right and left wheel motor respectively, d is the distance from the rear axle to the front of the robot.

$$\bar{\boldsymbol{M}} = \begin{bmatrix} m & 0 \\ 0 & I - md^2 \end{bmatrix}, \bar{\boldsymbol{B}} = \frac{1}{r}\begin{bmatrix} 1 & 1 \\ R & -R \end{bmatrix}, \bar{\boldsymbol{C}} = \begin{bmatrix} 0 & 0 \\ 0 & 0 \end{bmatrix}, \boldsymbol{X} = \frac{1}{r}\begin{bmatrix} 1 & R \\ 1 & -R \end{bmatrix}$$

Where m is the mass of the WMR, I is the moment of inertia of the WMR about its center, $\boldsymbol{X}$ is the generalized velocity around the driving wheel speed relationship matrix, $a_1 = N^2K_TK_b / R_a$ and $a_2 = NK_T / R_a$ as parameters, N is the gear ratio, K_T is the torque constant, R_a is the motor resistance, K_b is the velocity constant.

3. Leader-follower Formation Control

The two popular techniques in leader-follower formation control include separation-separation and separation-bearing, the later is used in this paper. Figure 1 shows the relative distance l_{ij} of two leader-follower robot system by nonholonomic constraints. The goal of separation-bearing formation control is to find a velocity input such that [4]:

$$\lim_{t\to\infty}(l_{ijd} - l_{ij}) = 0, \quad \lim_{t\to\infty}(\psi_{ijd} - \psi_{ij}) = 0 \quad (3)$$

Where l_{ij} and ψ_{ij} are the measured separation and bearing of the follower robot with l_{ijd} and ψ_{ijd} represent desired distance and angles respectively.

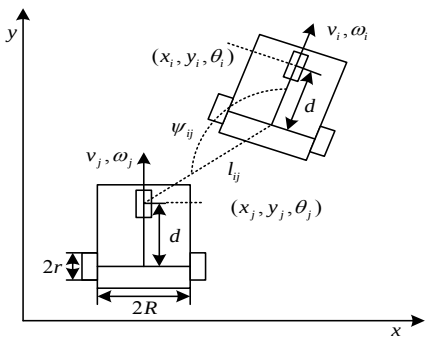

Figure 1. Leader-follower Robot System

3.1. Tracking Control of Leader-follower

To complete separation-bearing formation control, single-robot control frameworks such as [10] were extended to leader-follower formation control. Then, a reference position at a desired separation l_{ijd} and bearing ψ_{ijd} for follower j with respect to the rear of leader i was defined, and the kinematic error system was found to be [8].

$$\boldsymbol{q}_{e_j} = \begin{bmatrix} e_{j1} \\ e_{j2} \\ e_{j3} \end{bmatrix} = \begin{bmatrix} l_{ijd}\cos(\psi_{ijd}+\theta_{ij}) - l_{ij}\cos(\psi_{ij}+\theta_{ij}) \\ l_{ijd}\sin(\psi_{ijd}+\theta_{ij}) - l_{ij}\sin(\psi_{ij}+\theta_{ij}) \\ \theta_{jr}-\theta_j \end{bmatrix} \tag{4}$$

Where $\theta_{ij} = \theta_i - \theta_j$, θ_{jr} is reference orientation, satisfy the following equation:

$$\dot{\theta}_{jr} = (\omega_i l_{ijd}\cos(\psi_{ijd}+\theta_{ij}) + v_i\sin(\theta_{ijr}) + k_{j2}e_{j2})/d_j \tag{5}$$

Where $\theta_{ijr} = \theta_i - \theta_{jr} \in [-\pi,\pi]$, $\dot{l}_{ij}$ and $\dot{\psi}_{ij}$ are defined as follows:

$$\begin{aligned} \dot{l}_{ij} &= v_j\cos\gamma_j - v_i\cos\psi_{ij} + d_j\omega_j\sin\gamma_j \\ \dot{\psi}_{ij} &= (v_i\sin\psi_{ij} - v_j\sin\gamma_j + d_j\omega_j\cos\gamma_j - l_{ij}\omega_i)/l_{ij} \end{aligned} \tag{6}$$

Where $\gamma_j = \psi_{ij} + \theta_{ij}$, the differential equation of (4) as follow:

$$\begin{bmatrix} \dot{e}_{j1} \\ \dot{e}_{j2} \\ \dot{e}_{j3} \end{bmatrix} = \begin{bmatrix} -v_j + v_i\cos\theta_{ij} + \omega_j e_{j2} - \omega_i l_{ijd}\sin\gamma_{jd} \\ -\omega_j e_{j1} + v_i\sin\theta_{ij} - d_j\omega_j + \omega_i l_{ijd}\cos\gamma_{jd} \\ \dot{\theta}_{jr} - \omega_j \end{bmatrix} \tag{7}$$

Where $\gamma_{jd} = \psi_{ijd} + \theta_{ij}$, e_{j1}, e_{j2}, e_{j3} represent pose tracking deviation of leader-follower system, v and ω represent linear and angular velocities, respectively; the subscript i, j represent the leader and the follower, respectively. d_j is the distance from the rear axle of follower to the front of the robot.

In order to stabilization kinematic system, so that the follower robot j has reached the position and orientation with respect to the leader i, the speed control input of the following have been proposed in [8]:

$$\boldsymbol{V}_{jc} = \begin{bmatrix} v_{jc} \\ \omega_{jc} \end{bmatrix} = \begin{bmatrix} v_i\cos\theta_{ij} + k_{j1}e_{j1} - \omega_i l_{ijd}\sin\gamma_{jd} \\ \dot{\theta}_{jr} + k_{j3}e_{j3}/d_j \end{bmatrix} \tag{8}$$

Where $\boldsymbol{k}_j = [k_{j1} \quad k_{j2} \quad k_{j3}]^T$ is a vector of positive constant.

Assumption 1. Follower j is equipped with sensors capable of measuring the separation distance l_{ij} and bearing ψ_{ij} and that both leader and follower are equipped with instruments to measure their linear and angular velocities as well as there orientations θ_i and θ_j.

Assumption 2. Wireless communication is available between the j^{th} follower and i^{th} leader with communication delays being zero.

Assumption 3. The i^{th} leader communicates its linear and angular velocities as well as its orientation to its j^{th} follower.

Assumption 4. The reference linear and angular velocities measured from the leader i are bounded.

3.2. Formation Adaptive Control

Define the velocity tracking error as:

$$\boldsymbol{e}_{jc} = \begin{bmatrix} e_{jc1} \\ e_{jc2} \end{bmatrix} = \boldsymbol{V}_{jc} - \boldsymbol{V}_j = \begin{bmatrix} v_{jc} - v_j \\ \omega_{jc} - \omega_j \end{bmatrix} \tag{9}$$

Based on backstepping thought, the error dynamics (7) can be transformed into:

$$\begin{bmatrix} \dot{e}_{j1} \\ \dot{e}_{j2} \\ \dot{e}_{j3} \end{bmatrix} = \begin{bmatrix} \omega_j e_{j2} - k_{j1} e_{j1} + e_{jc1} \\ -k_{j2} e_{j2} - k_{j3} e_{j3} - \omega_j e_{j1} + d_j e_{jc2} + \mu_j \\ -k_{j3} e_{j3} / d_j + e_{jc2} \end{bmatrix} \tag{10}$$

Where $\mu_j = 2v_i \sin(e_{j3}/2)\cos(\theta_i - (\theta_{jr} + \theta_j)/2)$, Derivative of the formula (9), and in the equation ends multiplied by $\bar{\boldsymbol{M}}$, And in the formula right end subtraction, add $a_1 \bar{\boldsymbol{B}} \boldsymbol{X} \boldsymbol{V}_{jc}$,

$$\bar{\boldsymbol{M}} \dot{\boldsymbol{e}}_{jc} = -a_{j1} \bar{\boldsymbol{B}} \boldsymbol{X} \boldsymbol{e}_{jc} + \boldsymbol{f}_j + a_{j1} \bar{\boldsymbol{B}} \boldsymbol{X} \boldsymbol{V}_{jc} - a_{j2} \bar{\boldsymbol{B}} \boldsymbol{u}_j \tag{11}$$

Where $\boldsymbol{f}_j = \begin{bmatrix} f_{j1} \\ f_{j2} \end{bmatrix} = \bar{\boldsymbol{F}}_j + \bar{\boldsymbol{\tau}}_{dj} + \begin{bmatrix} a_{j3} \dot{v}_c \\ a_{j4} \dot{\omega}_c \end{bmatrix}$, $a_{j4} = I - md^2$, $a_{j3} = m$, Along with the load change, m and I are variable. In order to make the followers tracking the reference trajectory and speed, and stabilization system (11) in the origin, In accordance with the principle of feedback linearization, the ideal controller $\boldsymbol{u}_j^*$ may take for:

$$\boldsymbol{u}_j^* = \alpha_{j1} \boldsymbol{X} \boldsymbol{V}_{jc} + \alpha_{j2} \bar{\boldsymbol{B}}^{-1} (\boldsymbol{\varpi}_j + \boldsymbol{f}_j) \tag{12}$$

Where $\boldsymbol{\varpi}_j = \begin{bmatrix} k_{j2} e_{j1} \\ d_j (k_{j2} e_{j2} + k_{j3} e_{j3}) \end{bmatrix}$, $\alpha_{j1} = a_{j1} / a_{j2} = NK_b$, $\alpha_{j2} = 1/a_{j2} = R_a / NK_T$, the uncertainty of $\boldsymbol{f}_j$, can use RBFNN approached,

$$\begin{bmatrix} f_{j1} \\ f_{j2} \end{bmatrix} = \begin{bmatrix} \boldsymbol{W}_{j1}^T \boldsymbol{H}_{j1}(\boldsymbol{x}_j) \\ \boldsymbol{W}_{j2}^T \boldsymbol{H}_{j2}(\boldsymbol{x}_j) \end{bmatrix} + \boldsymbol{\varepsilon}_j \tag{13}$$

Where $\boldsymbol{x}_j = \left[e_{jc1}, e_{jc2}, \dot{v}_{jc}, \dot{\omega}_{jc} \right]^T$ for RBFNN input, $\boldsymbol{\varepsilon}_j$ is a neural network approximation error, $\left\| \boldsymbol{\varepsilon}_j \right\| \le \rho_j$, $\boldsymbol{W}_1$ and $\boldsymbol{W}_2$ is the weight vector of the neural network. In order to get dynamic approximation uncertainties $\boldsymbol{f}_j$, the estimated value $\hat{\boldsymbol{W}}_1$ and $\hat{\boldsymbol{W}}_2$ instead of the original value.

$$\hat{\boldsymbol{f}}_j = \begin{bmatrix} \hat{f}_{j1} \\ \hat{f}_{j2} \end{bmatrix} = \begin{bmatrix} \hat{\boldsymbol{W}}_{j1}^T \boldsymbol{H}_{j1}(\boldsymbol{x}_j) \\ \hat{\boldsymbol{W}}_{j2}^T \boldsymbol{H}_{j2}(\boldsymbol{x}_j) \end{bmatrix} \tag{14}$$

Using robust compensation term approximation error, we can get new controller is as follows:

$$\boldsymbol{u}_j = \alpha_{j1} \boldsymbol{X} \boldsymbol{V}_{jc} + \alpha_{j2} \bar{\boldsymbol{B}}^{-1} \left\{ \boldsymbol{\varpi}_j + \hat{\boldsymbol{f}}_j + \hat{\rho}_j \cdot sign(\boldsymbol{e}_{jc}) \right\} \tag{15}$$

Where, $\hat{\rho}_j$ is the estimate of ρ_j.

Theorem 1. Given kinematic equation of (1) and dynamic equation including actuator dynamics of (2) for follower *j*, along with the leader follower criterion of (3), leader-follower formation

model (6). Letting Assumption 1-4 hold, we select the speed control input (8), the drive voltage controller (15), the neural network weights update law (16), (17), and parameter adaptive law (18). Then $\boldsymbol{e}_j$, $\boldsymbol{e}_{jc}$, $\tilde{\boldsymbol{W}}_j$ and $\tilde{\rho}_j$ which are the position, orientation, velocity tracking errors, and the NN weight estimates as well as robust gain deviation for follower j are UUB, therefore, the robot formation system is asymptotically stable. Robot formation system is locally asymptotically stable.

$$\dot{\tilde{\boldsymbol{W}}}_{j1} = \dot{\hat{\boldsymbol{W}}}_{j1} = \eta_{j1} e_{jc1} \boldsymbol{H}_{j1}(\boldsymbol{x}_j) \tag{16}$$

$$\dot{\tilde{\boldsymbol{W}}}_{j2} = \dot{\hat{\boldsymbol{W}}}_{j2} = \eta_{j1} e_{jc2} \boldsymbol{H}_{j2}(\boldsymbol{x}_j) \tag{17}$$

$$\dot{\hat{\rho}}_j = \dot{\tilde{\rho}}_j = \eta_{j3} \left\| \boldsymbol{e}_{jc} \right\| \tag{18}$$

Where $\tilde{\boldsymbol{W}}_{j1} = \hat{\boldsymbol{W}}_{j1} - \boldsymbol{W}_{j1}$, $\tilde{\boldsymbol{W}}_{j2} = \hat{\boldsymbol{W}}_{j2} - \boldsymbol{W}_{j2}$, the value of η_{j1} and η_{j2} for the right gain, $\tilde{\rho}_j = \hat{\rho}_j - \rho_j$, η_{j3} is parameter adaptive law gain.

Proof: Choose the following Lyapunov function:

$$L_j = L_{j1} + L_{j2} \tag{19}$$

$$L_{j1} = \frac{k_{j2}(e_{j1}^2 + e_{j2}^2)}{2} + \frac{d_j k_{j3} e_{j3}^2}{2} \tag{20}$$

$$L_{j2} = \frac{1}{2}(\boldsymbol{e}_{jc}^T \bar{\boldsymbol{M}} \boldsymbol{e}_{jc} + \eta_{j1}^{-1} \tilde{\boldsymbol{W}}_{j1}^T \tilde{\boldsymbol{W}}_{j1} + \eta_{j2}^{-1} \tilde{\boldsymbol{W}}_{j2}^T \tilde{\boldsymbol{W}}_{j2} + \eta_{j3}^{-1} \tilde{\rho}_j^2) \tag{21}$$

Take the derivation for (19) and substitute (10), (15)-(18) in $\dot{L}_j$, we can obtain:

$$\begin{aligned} \dot{L}_j = \dot{L}_{j1} + \dot{L}_{j2} &= -k_{j1} k_{j2} e_{j1}^2 - k_{j2}^2 e_{j2}^2 - k_{j2}^2 e_{j3}^2 + 2k_{j2} e_{j2} v_i \sin(e_{j3}/2) \cos(\theta_i - (\theta_{jr} + \theta_j)/2) \\ &\quad - k_{j2} k_{j3} e_{j2} e_{j3} - a_{j1} \boldsymbol{e}_{jc}^T \bar{\boldsymbol{B}} \boldsymbol{X} \boldsymbol{e}_{jc} + \boldsymbol{e}_{jc}^T \boldsymbol{\varepsilon}_j - \rho_j \left\| \boldsymbol{e}_{jc} \right\| - \tilde{\boldsymbol{W}}_{j1}^T \left[e_{jc1} \boldsymbol{H}_{j1}(\boldsymbol{x}_j) - \eta_{j1}^{-1} \dot{\hat{\boldsymbol{W}}}_{j1}^T \right] \\ &\quad - \tilde{\boldsymbol{W}}_{j2}^T \left[e_{jc2} \boldsymbol{H}_{j2}(\boldsymbol{x}_j) - \eta_{j2}^{-1} \dot{\hat{\boldsymbol{W}}}_{j2}^T \right] \\ &= -k_{j1} k_{j2} e_{j1}^2 - k_{j2}^2 e_{j2}^2 - k_{j2}^2 e_{j3}^2 - k_{j2} k_{j3} e_{j2} e_{j3} + 2k_{j2} e_{j2} v_i \sin(e_{j3}/2) \cos(\theta_i - (\theta_{jr} + \theta_j)/2) \\ &\quad - a_{j1} \boldsymbol{e}_{jc}^T \bar{\boldsymbol{B}} \boldsymbol{X} \boldsymbol{e}_{jc} + \boldsymbol{e}_{jc}^T \boldsymbol{\varepsilon}_j - \rho_j \left\| \boldsymbol{e}_{jc} \right\| \end{aligned} \tag{22}$$

By $e_{j3} \in [-\pi, \pi]$, get $\left|\sin(e_{j3}/2)\right| \le \left|e_{j3}\right|$, then

$$\dot{L}_j \le -k_{j1} k_{j2} e_{j1}^2 - k_{j2}^2 e_{j2}^2 - k_{j2}^2 e_{j3}^2 - a_{j1} \boldsymbol{e}_{jc}^T \bar{\boldsymbol{B}} \boldsymbol{X} \boldsymbol{e}_{jc} + k_{j2} \left| e_{j2} e_{j3} \right| (k_{j3} + 2v_{i\max}) + \left\| \boldsymbol{e}_{jc} \right\| \left\| \boldsymbol{\varepsilon}_j \right\| - \rho_j \left\| \boldsymbol{e}_{jc} \right\| \tag{23}$$

By choosing k_{j3} get $2v_{i\max} < k_{j3}$, $\forall \varepsilon_{vj} > 0$, to ensure that the above inequality is established, select $k_{j3} = 2v_{i\max} + \varepsilon_{vj}$, by selecting $\varepsilon_{vj} = 2\varepsilon_{k3} k_{j3}$, when $\varepsilon_{k3} \in (0, 1/2)$, make $k_{j3} = 2v_{i\max} / (1 - 2\varepsilon_{k3})$, then

$$\dot{L}_j \le -k_{j1} k_{j2} e_{j1}^2 - \varepsilon_{k3} k_{j2}^2 e_{j2}^2 - \varepsilon_{k3} k_{j2}^2 e_{j3}^2 - (1 - \varepsilon_{k3})(k_{j3} \left| e_{j3} \right| - k_{j2} \left| e_{j2} \right|)^2 - a_{j1} \boldsymbol{e}_{jc}^T \bar{\boldsymbol{B}} \boldsymbol{X} \boldsymbol{e}_{jc} + \left\| \boldsymbol{e}_{jc} \right\| (\left\| \boldsymbol{\varepsilon}_j \right\| - \rho_j) \le 0 \tag{24}$$

Obviously through the selection of parameters can ensure the former four item of $\dot{L}_j$ is negative, therefore:

$$\dot{L}_j \le -a_{j1}\boldsymbol{e}_{jc}^T\bar{\boldsymbol{B}}\boldsymbol{X}\boldsymbol{e}_{jc} + \left\|\boldsymbol{e}_{jc}\right\|(\left\|\boldsymbol{\varepsilon}_j\right\| - \rho_j) \le 0 \tag{25}$$

Then define the following term:

$$p(t) = a_{j1}\boldsymbol{e}_{jc}^T\bar{\boldsymbol{B}}\boldsymbol{X}\boldsymbol{e}_{jc} + (\rho_j - \left\|\boldsymbol{\varepsilon}_j\right\|)\left\|\boldsymbol{e}_{jc}\right\| = -\dot{L}_{j2} \tag{26}$$

Because L_{j2} is non-increasing and bounded, we can obtain:

$$\int_0^t p(\tau)d\tau \le L_{j2}(\boldsymbol{e}_{jc}(0), \tilde{\rho}_j(0)) - L_{j2}(\boldsymbol{e}_{jc}(t), \tilde{\rho}_j(t)) \tag{27}$$

Also, because p is bounded, it can shown that $\lim_{t\to\infty} p(t) = 0$ by Barbalat's Lemma. We have $\lim_{t\to\infty}\boldsymbol{e}_{jc}(t) = 0$. Through the auxiliary speed control input (9) can guarantee pose deviation $\boldsymbol{q}_{e_j}$ are close to zero. Therefore, through the parameter design, you can ensure that pose deviation $\boldsymbol{q}_{e_j}$, speed tracking error $\boldsymbol{e}_{jc}$, neural network weights estimation error $\tilde{\boldsymbol{W}}_{j1}$, $\tilde{\boldsymbol{W}}_{j2}$, robust gain deviation $\tilde{\rho}_j$ are UUB. Robot formation system is locally asymptotically stable. This completes the proof of the theorem.

3.3. Leader Control Structure

Assumption 5. Leader tracks the virtual robot trajectory.

Assumption 6. The formation leader is capable of measuring its absolute position via instrumentation like GPS so that tracking the virtual robot is possible.

The kinematics and dynamics of the formation leader i are defined similarly to (1) and (2) respectively. From [10], the leader tracks a virtual reference robot, and the control velocity $\boldsymbol{V}_{ic}$ can be defined as follows:

$$\boldsymbol{V}_{ic} = \begin{bmatrix} v_{ic} \\ \omega_{ic} \end{bmatrix} = \begin{bmatrix} v_{ir}\cos e_{i3} + k_{i1}e_{i1} \\ \omega_{ir} + k_{i2}v_{ir}e_{i2} + k_{i3}v_{ir}\sin e_{i3} \end{bmatrix} \tag{28}$$

Where, $k_{ib}(b = 1,2,3)$ is a positive constant.

Defining the error system for leader i using similar steps for follower j:

$$\boldsymbol{e}_{ic} = \begin{bmatrix} e_{ic1} \\ e_{ic2} \end{bmatrix} = \boldsymbol{V}_{ic} - \boldsymbol{V}_i \tag{29}$$

The input voltage control for leader i can be defined similarly to follower j's as follow:

$$\boldsymbol{u}_i = \alpha_{i1}\boldsymbol{X}\boldsymbol{V}_{ic} + \alpha_{i2}\bar{\boldsymbol{B}}^{-1}\left\{\boldsymbol{\varpi}_i + \hat{\boldsymbol{f}}_i + \hat{\rho}_i \cdot sign(\boldsymbol{e}_{ic})\right\} \tag{30}$$

Where $\boldsymbol{\varpi}_i = \begin{bmatrix} e_{i1} \\ (\sin e_{j3})/k_{i2} \end{bmatrix}$, $\hat{\boldsymbol{f}}_i = \begin{bmatrix} \hat{f}_{i1} \\ \hat{f}_{i2} \end{bmatrix} = \begin{bmatrix} \hat{\boldsymbol{W}}_{i1}^T\boldsymbol{H}_{i1}(\boldsymbol{x}_i) \\ \hat{\boldsymbol{W}}_{i2}^T\boldsymbol{H}_{i2}(\boldsymbol{x}_i) \end{bmatrix}$, $\boldsymbol{x}_i = \left[e_{ic1}, e_{ic2}, \dot{v}_{ic}, \dot{\omega}_{ic}\right]^T$, $\hat{\rho}_i$ is the estimate of ρ_i.

Theorem 2. Given kinematic equation of (1) and dynamic equation including actuator dynamics of (2) for leader i, letting Assumption 5-6 hold, we can select kinematic speed controller (28), the drive voltage controller (30), the neural network weights update law (31), (32), parameter adaptive law (33). Then $\boldsymbol{e}_i$, $\boldsymbol{e}_{ic}$, $\tilde{\boldsymbol{W}}_i$ and $\tilde{\rho}_i$ which are the position, orientation, velocity tracking errors, and the NN weight estimates as well as robust gain deviation for leader j are UUB, therefore, the leader robot system is asymptotically stable.

$$\dot{\tilde{\boldsymbol{W}}}_{i1} = \dot{\hat{\boldsymbol{W}}}_{i1} = \eta_{i1} e_{ic1} \boldsymbol{H}_{i1}(\boldsymbol{x}_i) \tag{31}$$

$$\dot{\tilde{\boldsymbol{W}}}_{i2} = \dot{\hat{\boldsymbol{W}}}_{i2} = \eta_{i2} e_{ic2} \boldsymbol{H}_{i2}(\boldsymbol{x}_i) \tag{32}$$

$$\dot{\hat{\rho}}_i = \dot{\tilde{\rho}}_i = \eta_{i3} \left\| \boldsymbol{e}_{ic} \right\| \tag{33}$$

Where $\tilde{\boldsymbol{W}}_{i1} = \hat{\boldsymbol{W}}_{i1} - \boldsymbol{W}_{i1}$, $\tilde{\boldsymbol{W}}_{i2} = \hat{\boldsymbol{W}}_{i2} - \boldsymbol{W}_{i2}$, the value of η_{i1} and η_{i2} for the right gain, $\tilde{\rho}_i = \hat{\rho}_i - \rho_i$, η_{i3} is parameter adaptive law gain.

Proof: Choose the following Lyapunov function:

$$L_i = L_{i1} + L_{i2} \tag{34}$$

$$L_{i1} = \frac{1}{2}(e_{i1}^2 + e_{i2}^2) + \frac{1 - \cos e_{i3}}{k_{i2}} \tag{35}$$

$$L_{i2} = \frac{1}{2}(\boldsymbol{e}_{ic}^T \bar{\boldsymbol{M}} \boldsymbol{e}_{ic} + \eta_{i1}^{-1} \tilde{\boldsymbol{W}}_{i1}^T \tilde{\boldsymbol{W}}_{i1} + \eta_{i2}^{-1} \tilde{\boldsymbol{W}}_{i2}^T \tilde{\boldsymbol{W}}_{i2} + \eta_{i3}^{-1} \tilde{\rho}_i^2) \tag{36}$$

The proof is similar to theorem 1, slightly.

4. Results and Analysis

The general structure of the mobile robot formation adaptive control including drive dynamics is shown in Figure 2. A wedge formation of three identical nonholonomic mobile robots is considered where the leader's trajectory is the desired formation trajectory and simulations are carried out in MATLAB. A simple wedge formation is considered such that follower j should track its leader at separation of $l_{ijd} = 2$ meters and a bearing of $\psi_{ijd} = \pm 120°$ depending on the follower's location, and the formation leader is located at the apex of the wedge. The following robotic parameters are considered for the leader and its followers: $R = 0.153\text{m}$, $N = 4$, $R_a = 2$, $K_b = 0.2$, $k_T = 0.5$, $m = 4\text{kg}$, $I = 2.5\text{kgm}^2$, $r = 0.03\text{m}$, $d = 0.25\text{m}$. The change of mobile robot's loads causes the change of parameters when the time of running lasts for five seconds: $m = 6\,\text{kg}$, $I = 4\text{kgm}^2$. Under both scenarios , unmodeled dynamics are introduced in the form of friction as: $\boldsymbol{F} = [\mu_1 sign(v) + \mu_2 v \quad \mu_3 sign(\omega) + \mu_4 \omega]^T$, where $\mu_i (i = 1, \cdots 4)$ varied between 0 and 1 for each robot. The suffered external disturbance of the mobile robot in the system is $\bar{\boldsymbol{\tau}}_d = 0.1 \cdot [\sin(t-8) \quad \sin(t-8)]^T$. Assuming uncertainties of the load changes, friction, and external interference in the formation of each robot. The following parameters are used for the controllers:

Leader i : $k_{i1} = 12$, $k_{i2} = 11$, $k_{i3} = 6.65$, $\eta_{i1} = 0.01$, $\eta_{i2} = 0.01$; $\eta_{i3} = 0.01$; follower j : $k_{j1} = 5$, $k_{j2} = 5$, $k_{j3} = 15$, $\eta_{j1} = 0.01$, $\eta_{j2} = 0.01$, $\eta_{j3} = 0.01$.

RBF neural network modeling uncertain part of the leader and followers take the same parameters, as follows: the number of hidden units is taken as 7. The values of the center c of Gaussian basis function are selected as the uniform according to interval 5. Variance σ is taken as 8, the rest of the initial values are 0. Original position deviations of leader take form $[1 \quad 0 \quad pi/4]$.

Divided into the following two cases simulation study: the first case, formation leader with the following speed, angular velocity and orientation tracking part of the right-angled trajectory:

$$\begin{cases} v_r = 5\,\text{m/s} & 0\text{s} \le t < 8\text{s} \\ v_r = 2\,\text{m/s} & 8\text{s} \le t \le 10\text{s} \\ \omega_r = 0\,\text{rad/s} & 0\text{s} \le t \le 10\text{s} \end{cases}, \quad \begin{cases} \theta_r = 0\,\text{rad} & 0\text{s} \le t < 3\text{s} \\ \theta_r = \dfrac{\pi}{2}\,\text{rad} & 3\text{s} \le t < 6\text{s} \\ \theta_r = \pi\,\text{rad} & 6\text{s} \le t \le 10\text{s} \end{cases}$$

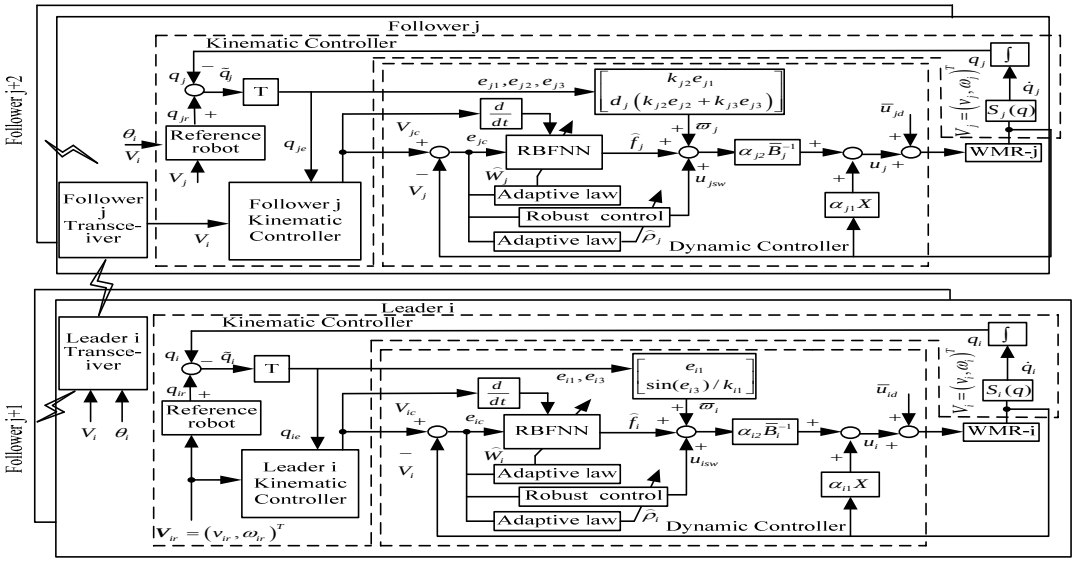

Figure 2. The General Structure of the Mobile Robot Formation Adaptive Control Including Drive Dynamics

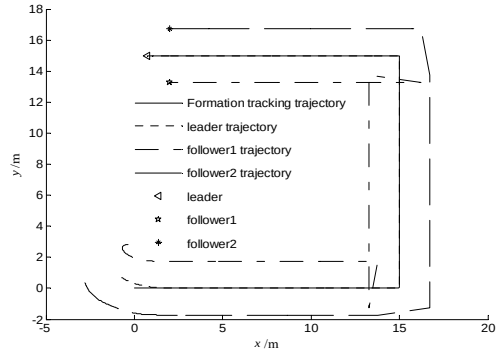

Figure 3. Triangle Formation Tracking Angle Trajectory

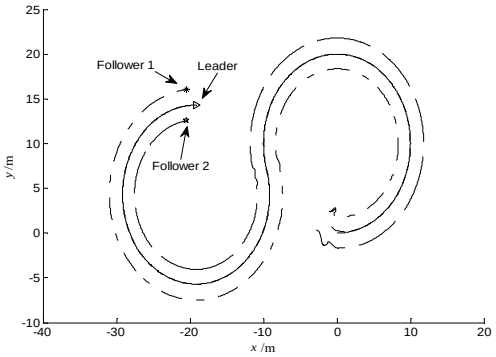

Figure 4. Trajectory Tracking of Triangle Formation

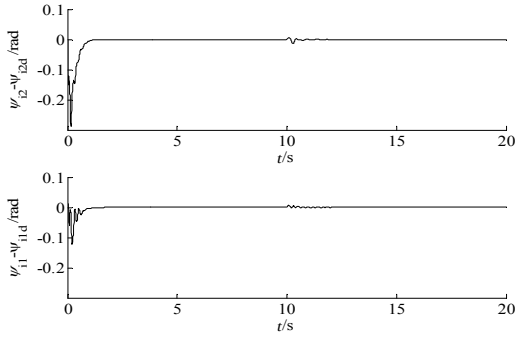

Figure 5. Tracking Errors of Relative Orientation from Follower to Leader

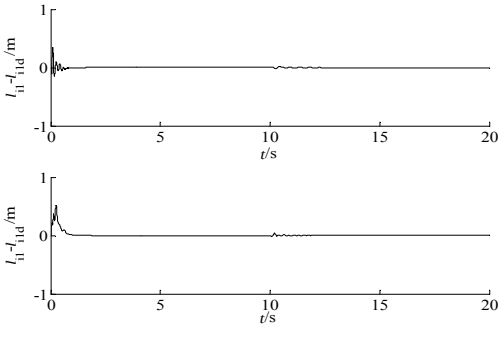

Figure 6. Tracking Errors of Relative Distance from Follower to Leader

The triangle formation on the right angle trajectory tracking of nonholonomic mobile robots is shown in Figure 3. The second case, formation leader tracking the trajectory of an S-type, in accordance with the following speed and angular velocity.

$$v_r = 5m/s, \quad \omega_r = \begin{cases} 0.5rad/s & t \le 10s \\ -0.5rad/s & t > 10s \end{cases}$$

The triangle formation on the S-shaped trajectory tracking of nonholonomic mobile robots is shown in Figure 4–Figure 6.

From Figure 3 and Figure 4, we can find that the algorithm is able to overcome many kinds of uncertainty factors in the system, and can better to achieve the tracking control of the reference trajectory. With reference to Figure 5 and Figure 6 can be seen that the follower robot and the leader robot can quickly reach the desired relative distance and relative orientation. Even in the case of the leader angular velocity suddenly reverse the formation through a brief correction, relative distance and relative orientation of the deviation of the follower and leader can quickly approaches zero, which maintains the desired formation for completing the trajectory tracking control. The results show that, at the same time existing load change, friction and external interference, the algorithm of a nonholonomic mobile robot formation trajectory tracking control is effective.

5. Conclusion

We studies the formation control problem of multiple nonholonomic mobile robots including actuator. This control law was designed by backstepping technique based on separation-bearing formation control structure of leader-follower. Robots in the formation (including the leader and followers) are the presence of all kinds of uncertainties such as load changes, interference and friction. A wedge formation of three identical nonholonomic mobile robots is considered, and simulations are carried out in MATLAB. The simulation results showed the effectiveness of this proposed method. This method not only solved the problem of parameters and non-parameter uncertainties of mobile robots, but also ensured the desired trajectory tracking of robot formation in the case of maintaining formation. The algorithm can also be used for single nonholonomic robot and other types of formation control, such as wedge, horizontal or vertical formation. For the dynamics parameters of the drive which is unknown will be the content of the further study.

Acknowledgment

This work was supported by the Program for Young Teachers Scientific Research in Qiqihar University under grant no. 2011k-M02, and the Program for the Natonal Natural Science Foundation of China under grant no.61100103.

References

[1] Balch T, Arkin RC. Behavior-based Formation Control for Multi-robot Teams. *IEEE Transactions on Robotics and Automation*. 1998; 14(6): 926–939.
[2] Lewis MA, Tan KH. High Precision Formation Control of Mobile Robots Using Virtual Structures. *Autonomous Robots*. 1997; 4(4): 387–403.
[3] Tanner HG, Pappas GJ, Kumar V. Leader-to-formation Stability. *IEEE Transactions on Robotics and Automation*. 2004; 20(3): 443–455.
[4] Dierks T, Jagannathan S. *Control of Nonholonomic Mobile Robot Formations: Backstepping Kinematics into Dynamics*.Proceedings of the 16th IEEE International Conference on Control Applications Part of IEEE Multi-conference on Systems and Control. Singapore. 2007: 94-99.
[5] Das A, Fierro R, Kumar V, et al. A Vision-based Formation Control Framework. *IEEE Transactions on Robotics and Automation*. 2002; 18(5): 813–825.
[6] Li XH, Xiao J, Cai Z. *Backstepping-based Multiple-mobile Robots Formation Control*. Proceedings of the 2005 IEEE/RSJ International Conference on Intelligent Robots and Systems. Edmonton, Alta, Canada. 2005: 887–892.
[7] Do KD. Formation-tracking Control of Unicycle-type Mobile Robots with Limited Sensing Ranges. *IEEE Transactions on Control Systems Technology*. 2008; 16(3): 527–538.
[8] Dierks T, Jagannathan S. Neural Network Control of Mobile Robot Formations Using RISE Feedback. *IEEE Transactions on Systems, Man, and Cybernetics-PART B: Cybernetics.* 2009; 39(2): 332– 347.
[9] Tamoghna Das, Kar IN, Chaudhury S. Simple Neuron-based Adaptive Controller for A Nonholonomic Mobile Robot Including Actuator Dynamics. *Neurocomputing*. 2006; 29: 2140-2151.

[10] Fierro R, Lewis FL. Control of A Nonholonomic Mobile Robot Using Neural Networks. *IEEE Transactions on Neural Network*. 1998; 9(4): 589–600.